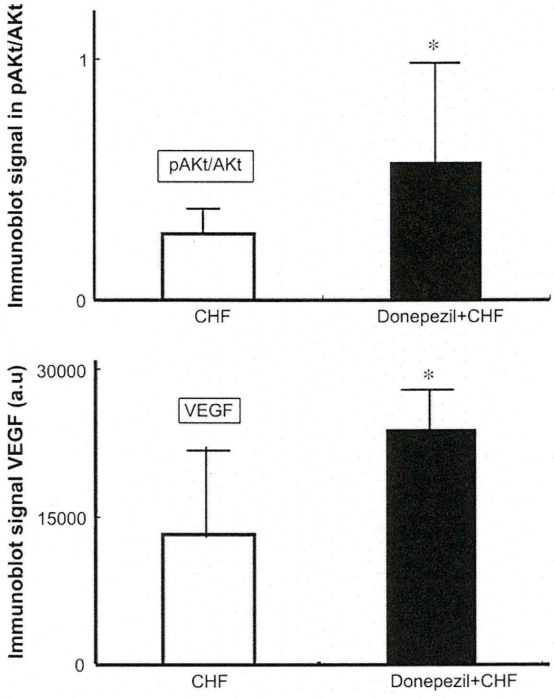

Fig. 1. Effects of donepezil on Akt phosphorylation and vascular endothelial growth factor (VEGF) expression in CHF mice. Each panel shows quantitative densitometric results from immunoblot analysis for left ventricles of untreated chronic heart failure (CHF) mice and donepezil-treated CHF mice (donepezil + CHF). Values are mean ± standard deviation (n = 7 for each group). a.u., arbitrary units. *$P < .05$ from CHF group.

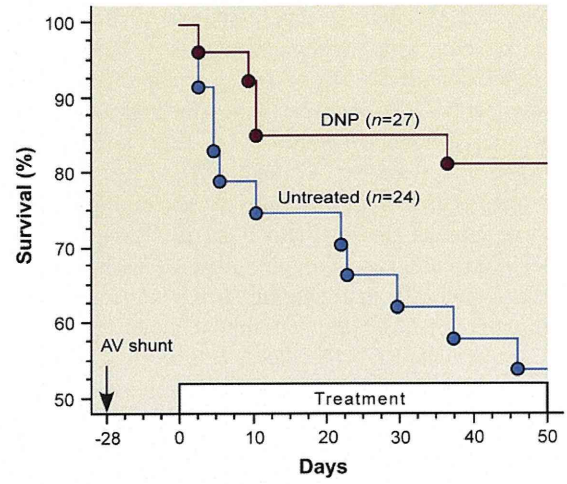

Fig. 2. Survival curves of chronic heart failure (CHF) mice with a large aortocaval (AV) shunt. At 4 weeks after the AV-shunt surgery, the survivors were randomized into untreated (blue line, n = 24) and donepezil-treated (red line, n = 27) groups. Donepezil treatment was continued for 50 days. The treatment significantly improved the survival rate ($P = .039$).

It is well known that a large dosage of donepezil has a bradycardiac effect on the vagally innervated heart through cholinesterase inhibition.[21,22] However, in the present study, this dosage of donepezil did not decrease HR in sham operative model, and then prevented the progression of CHF induced by large AV shunt. The present results suggest that the bradycardia induced by large AV shunt is prevented by donepezil. Similarly, our previous studies[2–4] showed that vagal nerve stimulation and ACh protected ventricular cardiomyocytes against ischemic and hypoxic insults through a different mechanism from its HR-slowing effect. Therefore, donepezil would have a cardioprotective effect independent of the HR-slowing mechanism. As our previous studies indicated, ACh released from vagal nerve stimulation inhibited hypoxia induced cell death through a PI3 K/Akt/hypoxia-inducible factor 1-α pathway, leading to cell survival,[3] and then, we showed that donepezil upregulated protein expression of phospho-Akt and VEGF, as shown in vagal nerve stimulation. Because the PI3 K/Akt pathway is one of the important cell survival signaling pathways[23]; therefore, the present results suggest that the beneficial effect of donepezil is derived from activation of cell survival pathways for prevention of CHF.

Donepezil was originally developed as a centrally acting inhibitor of acetylcholinesterase, and is available for the treatment of Alzheimer's disease.[24] Therefore, it is likely that the beneficial effects of donepezil on CHF resulted from its central actions. However, several in vitro studies also suggest that the neuroprotective actions of donepezil would be exerted principally by its pharmacological properties other than acetylcholinesterase inhibition.[25,26] Unlike peripherally acting cholinesterase inhibitors such as physostigmine and neostigmine, donepezil is reported to have a high affinity for σ receptors and to exhibit cytoprotective effects on neuronal cells via the σ receptor–related activation of intracellular choline acetyltransferase.[27] Although the presence of σ receptors has been also shown in cardiomyocytes of animals[28] and humans,[29] there is very little information available on the functional role of σ receptors in CHF. Therefore, further studies are needed for clarifying the mechanism of anti-CHF effects of the anti-Alzheimer's drug.

Limitations

The dosage of donepezil used in the present study was almost 50 times higher than that in clinical settings for the treatment of Alzheimer's disease. Therefore, it might be better to investigate whether or not the clinical dosage for donepezil also has a beneficial effect on CHF in mice comparably with the higher dose. However, despite of the lower dose for clinical application, in animal studies with donepezil, the daily dose of 5 mg/kg has been extensively used to exhibit a beneficial effect on dementia in a rodent model.[30] Auletta et al reported that the chronic oral daily dose larger than 10 mg/kg has adverse effects on food consumption, blood biochemistry, and urinalysis in rodents.[31]

Furthermore, our recent clinical investigation also has suggested the protective effect of chronic donepezil

treatment at 3 to 5 mg/day suppressed cardiovascular mortality in patients with Alzheimer's disease.[5] Moreover, the lower dosed donepezil still possess a cardioprotective effect on rat myocardial infarcted heart. Thus, the present results do not necessarily indicate that the dose of 5 $mg \cdot kg^{-1} \cdot day^{-1}$ is required for the treatment of human CHF.

The main objective of this study was to confirm the retrospective clinical finding[5] about the protective effect of donepezil on cardiovascular mortality, to simply test the working hypothesis that chronic donepezil can improve the prognosis of CHF with an animal model, and not to clarify the mechanism. Therefore, cellular and molecular mechanisms for the beneficial effects of donepezil are little clarified in the present study. To establish the therapeutic strategy, further investigation on action sites, dose-dependent effects, and adverse effects of donepezil on CHF is required. And other cholinesterase inhibitors had severe side effects and therapeutic range was reported to be narrow (0.1 to 0.3 mg/kg, intraperitoneally) for in vivo mice model,[32] unlike donepezil; therefore, we didn't perform further studies using those inhibitors.

Conclusion

The present study demonstrated that oral donepezil improved survival of CHF mice through prevention of pumping failure and cardiac remodeling. However, the mechanisms of anti-CHF actions of donepezil and the appropriate protocol for the treatment of CHF are still unsettled and should be investigated. To establish the therapeutic strategy shown in the present study, large-scale and long-term clinical trials are required as well as animal studies.

References

1. Li M, Zheng C, Sato T, Kawada T, Sugimachi M, Sunagawa K. Vagal nerve stimulation markedly improves long-term survival after chronic heart failure in rats. Circulation 2004;109:120–4.
2. Ando M, Katare RG, Kakinuma Y, Zhang D, Yamasaki F, Muramoto K, et al. Efferent vagal nerve stimulation protects heart against ischemia-induced arrhythmias by preserving connexin43 protein. Circulation 2005;112:164–70.
3. Kakinuma Y, Ando M, Kuwabara M, Katare RG, Okudela K, Kobayashi M, et al. Acetylcholine from vagal stimulation protects cardiomyocytes against ischemia and hypoxia involving additive non-hypoxic induction of HIF-1 alpha. FEBS Lett 2005;579:2111–8.
4. Katare RG, Ando M, Kakinuma Y, Arikawa M, Handa T, Yamasaki F, et al. Vagal stimulation prevents reperfusion injury through inhibition of opening of mitochondrial permeability transition pore independent of the bradycardiac effect. J Thorac Cardiovasc Surg 2008;137:223–31.
5. Sato K, Urbano R, Yu C, Yamasaki F, Sato T, Robertson D, et al. Protective effect of donepezil on cardiovascular mortality. [abstract]. Circulation 2008;117:e269.
6. Scheuermann-Freestone M, Freestone NS, Langenickel T, Höhnel K, Dietz R, Willenbrock R. A new model of congestive heart failure in the mouse due to chronic volume overload. Eur J Heart Fail 2001;3:535–43.
7. Sutherland FJ, Shattock MJ, Baker KE, Hearse DJ. Mouse isolated perfused heart: characteristics and cautions. Clin Exp Pharmacol Physiol 2003;30:867–78.
8. Sato T, Shishido T, Kawada T, Miyano H, Miyashita H, Inagaki M, et al. ESPVR of in situ rat left ventricle shows contractility-dependent curvilinearity. Am J Physiol Heart Circ Physiol 1998;274:H1429–34.
9. Kameyama T, Chen Z, Bell SP, Fabian J, Lewinter MM. Mechanoenergetic studies in isolated mouse hearts. Am J Physiol Heart Circ Physiol 1998;274:H366–74.
10. Claessens TE, Georgakopoulos D, Afanasyeva, Vermeersch SJ, Millar HD, et al. Nonlinear isochrones in murine left ventricular pressure-volume loops: how well does the time-varying elastance concept hold? Am J Physiol Heart Circ Physiol 2006;290:H1474–83.
11. Mirsky I, Tajimi T, Peterson KL. The development of the entire end-systolic pressure-volume and ejection fraction-afterload relations: a new concept of systolic myocardial stiffness. Circulation 1987;76:343–56.
12. Packer M, Coats AJ, Flowler MB, Katus HA, Krum H, Mohacsi P, et al. Carvedilol Prospective Randomized Cumulative Survival Study Group. Effect of carvedilol on survival in severe chronic heart failure. N Engl J Med 2001;344:1651–8.
13. Effect of enalapril on survival in patients with reduced left ventricular ejection fractions and congestive heart failure. The SOLVD Investigators. N Engl J Med 1991;325:293–302.
14. Pfeffer MA, Swedberg K, Granger CB, Held P, McMurray JJ, Michelson EL, et al. CHARM Investigators and Committees. Effects of candesartan on mortality and morbidity in patients with chronic heart failure: the CHARM-Overall programme. Lancet 2003;362:759–66.
15. Pitt B, Remme W, Zannad F, Neaton J, Martines F, Roniker B, et al. Eplerenone Post-Acute Myocardial Infarction Heart Failure Efficacy and Survival Study Investigators. Eplerenone, a selective aldosterone blocker, in patients with left ventricular dysfunction after myocardial infarction. N Engl J Med 2003;348:1309–21.
16. Shinke T, Takeuchi M, Takaoka H, Yokoyama M. Beneficial effects of heart rate reduction on cardiac mechanics and energetics in patients with left ventricular dysfunction. Jpn Circ J 1999;63:957–64.
17. Hu K, Naumann A, Fraccarollo D, Gaudron P, Kaden JJ, Neubauer S, et al. Heart rate reduction by zatebradine reduces infarct size and mortality but promotes remodeling in rats with experimental myocardial infarction. Am J Physiol Heart Circ Physiol 2004;286:H1281–8.
18. Nishikimi T, Hagaman JR, Takahashi N, Kim HS, Matsuoka H, Smithies O, et al. Increased susceptibility to heart failure in response to volume overload in mice lacking natriuretic peptide receptor-A gene. Cardiovasc Res 2005;66:94–103.
19. Cox MJ, Hawkins UA, Hoit BD, Tyagi SC. Attenuation of oxidative stress and remodeling by cardiac inhibitor of metalloproteinase protein transfer. Circulation 2004;109:2123–8.
20. Kamkin A, Kiseleva I, Wagner KD, Pylaev A, Leiterer KP, Theres H, et al. A possible role for atrial fibroblasts in postinfarction bradycardia. Am J Physiol Heart Circ Physiol 2002;282:H842–9.
21. Shepherd G, Klein-Schwartz W, Edwards R. Donepezil overdose: a tenfold dosing error. Ann Pharmacother 1999;33:812–5.
22. Bordier P, Garrigue S, Barold SS, Bressolles N, Lanusse S, Clémenty J. Significance of syncope in patients with Alzheimer's disease treated with cholinesterase inhibitors. Europace 2003;5:429–31.
23. Vanhaesebroeck B, Alessi DR. The regulation and activities of the multifunctional serine/threonine kinase Akt/PKB. Exp. Cell Res 1999;253:210–29.
24. Rogers SL. Perspectives in the management of Alzheimer's disease: clinical profile of donepezil. Dement Geriatr Cogn Disord 1998;9(Suppl 3):29–42.
25. Maurice T, Meunier J, Feng B, Ieni J, Monaghan DT. Interaction with $sigma_1$ protein, but not *N*-methyl-D-aspartate receptor, is involved in the pharmacological activity of donepezil. J Pharmacol Exp Ther 2006;317:606–14.
26. Meunier J, Ieni J, Maurice T. The anti-amnesic and neuroprotective effects of donepezil against amyloid $beta_{25-35}$ peptide-induced toxicity in mice involve an interaction with the $sigma_1$ receptor. Br J Pharmacol 2006;149:998–1012.

27. Kato K, Hayako H, Ishihara Y, Marui S, Iwane M, Miyamoto M. TAK-147, an acetylcholinesterase inhibitor, increases choline acetyltransferase activity in cultured rat septal cholinergic neurons. Neurosci Lett 1999;260:5–8.
28. Novakova M, Ela C, Barg J, Vogel Z, Hasin Y, Eilam Y. Inotropic action of sigma receptor ligands in isolated cardiac myocytes from adult rats. Eur J Pharmacol 1995;286:19–30.
29. Kekuda R, Prasad PD, Fei YJ, Leibach FH, Ganapathy V. Cloning and functional expression of the human type 1 sigma receptor (hSigmaR1). Biochem Biophys Res Commun 1996;229:553–8.
30. Saxena G, Singh SP, Agrawal R, Nath C. Effect of donepezil and tacrine on oxidative stress in intracerebral streptozotocin-induced model of dementia in mice. Eur J Pharmacol 2008;581:283–9.
31. Auletta CS, Mitchell JM, Richter WR, Taki T, Sagami F. One-year oral toxicity study of donepezil hydrochloride in rats. Jpn Pharmacol Ther 1998;26(Suppl 6):S1177–95.
32. Akinci SB, Ulu N, Yondem OZ, Firat P, Guc MO, Kanbak M, Aypar U. Effect of neostigmine on organ injury in murine endotoxemia: missing facts about the cholinergic anti-inflammatory pathway. World J Surg 2005;29:1483–9.

In the Spotlight: BioInstrumentation

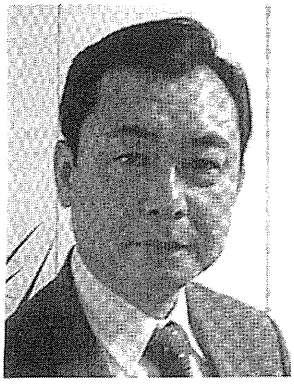

Ken-ichi Yamakoshi, *Member, IEEE*

I. Introduction

THE field of biomedical instrumentation continues to attract a considerable amount of research activity and effort worldwide in order to produce more convenient, reliable and useful apparatus for medical science. This covers numerous aspects of the field such as measurement principles and methodologies as well as transducers and instruments, with applications for diagnosis and/or health care. In this review, four topics are briefly introduced, based on recent publications in this area. These are: 1) ballistocardiography revisited; 2) current studies on noninvasive measurement of arterial blood pressure; 3) electrophysiological measurement with dry electrodes; and 4) recent advances in noninvasive optical measurement of blood constituents.

II. Ballistocardiography Revisited

Ballistocardiography is a measurement method based on the detection of the small change in body weight caused by the recoil of shifts in the center of mass of the blood ejected by ventricular contraction. The first report of the ballistocardiogram (BCG) measurement was in 1877 [1]. This is now considered as only a preliminary description, but, in 1936, Starr developed what is regarded as the epoch-making bed BCG measurement device [2]. Following this, many BCG studies were done over a three or four decade period, but, the use and study of BCG decreased in the latter half of the 1970s and then the method attracted little or no further scientific research interest in the field of biomedical engineering.

Manuscript received September 27, 2009; revised September 28, 2009. Current version published November 18, 2009.

K.-I. Yamakoshi is with the Graduate School of Natural Science & Technology, Kanazawa University, Kakuma, Kanazawa 920-1192, Japan (e-mail: yamakosi@t.kanazawa-u.ac.jp).

Digital Object Identifier 10.1109/RBME.2009.2034696

Ballistocardiography, however, is an attractive method due to the fact that it has the potential to allow truly noninvasive assessment of cardiac ejection function. This feature can be understood by considering the origin of the BCG as follows: As shown in Fig. 1(a), according to Newton's second law, the reaction force originating from blood ejection by ventricular contraction during the systolic period, $\boldsymbol{F(t)}$, i.e., the BCG, is a derivative of the momentum, $\boldsymbol{P(t)}$, $(\boldsymbol{F}(t) = d\boldsymbol{P}(t)/dt)$. The momentum, $\boldsymbol{P(t)}$, is the product of blood velocity, $\boldsymbol{v}(t)$, in the ascending aorta and the mass of ejected blood, $m(t)$, where $m(t)$ is the product of ejected blood volume, $V(t)$, and blood density coefficient, ρ, i.e., $\boldsymbol{m}(t) = \rho V(t)$. Therefore, $\boldsymbol{F}(t)$ can be expressed by $\boldsymbol{F}(t) = \rho d(\boldsymbol{v}(t)V(t))/dt$. Then $V(t)$ is derived by integration of $v(t)$ during systole, and thus $\boldsymbol{F}(t) = \rho d(\boldsymbol{v(t)} \int \boldsymbol{v}(t)dt)/dt$. If $\boldsymbol{v}(t)$ is given as shown in the top panel of Fig. 1(b), then $\boldsymbol{F}(t)$ can be calculated as shown in the bottom panel of Fig. 1(b). The pattern of the calculated $\boldsymbol{F}(t)$ is quite similar to the measured BCG during systole, as shown in Fig. 1(c). Thus it can be seen that the BCG can contain information about cardiac ejection function.

In fact, several studies on BCG measurement have been made in this decade for the assessment of cardiac function. For example, we recently developed a new BCG monitor using a weighing scale with high resolution and accuracy that was installed in a toilet. This has successfully demonstrated BCG measurements, as well as the evaluation of cardiac functions such as cardiac output (CO), during the use of the toilet [3], [4]. More recently, the interest in BCG measurement has increased and further studies have been made by several groups. Inan *et al.* reported BCG measurement using subjects in a standing position and demonstrated a relatively low-cost BCG monitor that was based on a commercial scale [5], [6]. They also tried to estimate CO changes derived from the BCG. Recordings of BCGs from subjects after treadmill exercise were made and compared with CO changes determined by Doppler echocardiogram signals from the left ventricular outflow tract of the

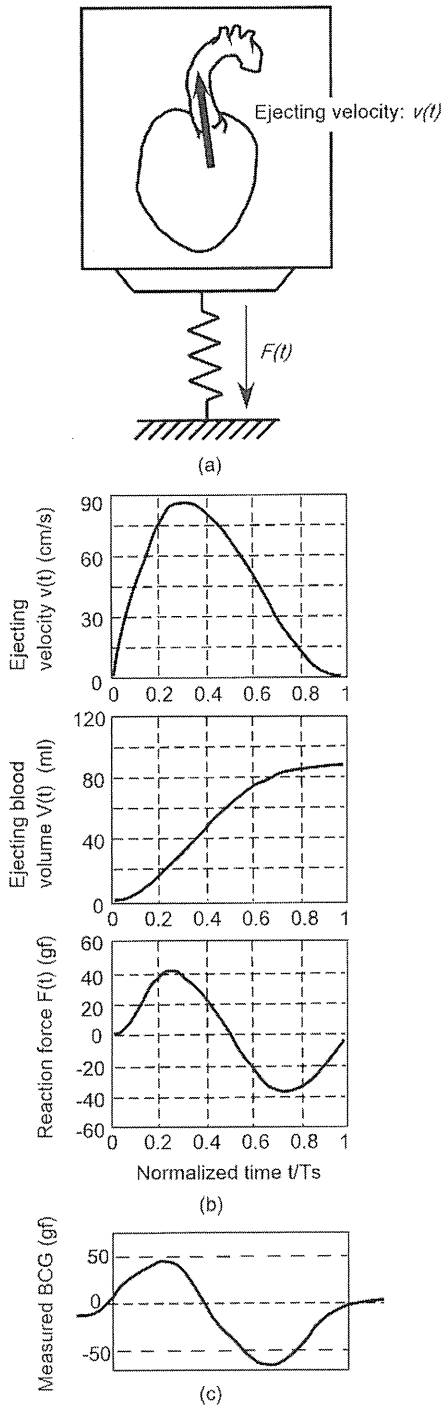

Fig. 1. Diagramatic representation of the origin of the ballistocardiogram (BCG) (a), an example of numerical simulation showing ejecting velocity ($v(t)$), ejecting blood volume (V (t)) and calculated reaction force ($F(t)$)(b), and an example of measured BCG (c). Abscissa in (b) indicates time (t) normalized by systolic period (Ts). See text for further explanation.

heart. The results showed a relatively good correlation between them [7]. Han *et al.* developed an enhanced chair-type BCG measurement device implemented in a wheelchair and demonstrated BCG monitoring together with ECG in a disabled person [8], [9]. Mack *et al.* tried to measure BCG signals in bed to assess heart rate during sleep using a force sensor placed beneath a bed sheet [10]. Chen *et al.* [11] and Motoi *et al.* [12] also demonstrated the BCG measurement during sleep using a flat-type sensor under a pillow.

Despite the increasing number of studies aimed at re-examining ballistocardiography, as described above, the method has still not become widely-accepted for clinical applications in the way that other methods such as ECG measurement have. Besides the need for new instruments using modern techniques, further clinical applications will need to be proven if the method is to recapture the past glory days.

III. Current Studies on Noninvasive Measurement of Arterial Blood Pressure

Noninvasive or indirect measurement of arterial blood pressure (BP) is an age-old topic and still of great importance in biomedical fields. Although several methods for noninvasive BP measurement have been proposed in the last two decades, validation studies against the gold standard of direct BP measurement with intra-arterial catheterization, have been lacking. Recently, Chemla *et al.* provided a review of recent advances in noninvasive BP measurement in the field of critical care [13]. These authors have drawn an important conclusion that in hemodynamically unstable patients when critical decisions are required direct BP measurement is preferred over noninvasive methods. Furthermore they also concluded that current commercially available BP instruments based on the auscultatory and/or cuff-oscillometric method may provide valuable information only for hemodynamically stable patients.

Advances in the field of noninvasive BP measurement are still required, either through further improvements to existing techniques or by means of entirely novel approaches. Within this context, Muehlsteff *et al.* tried to estimate BP by the use of a conventional pulse arrival time method [14]. Shin *et al.* reported the measurement of systolic BP from the BCG and compared the resulting BP values with those derived by Finapres, a commercially available BP monitor [15]. Suzuki *et al.* attempted to estimate BP by analyzing photoplethysmographic signals and the BP values were compared with those from a commercial cuff-oscillometric type BP monitor [16]. A new cuff-less BP measuring method based on hydrostatic pressure has been proposed by Shaltis *et al.*, results being compared with data from a Finapres monitor [17].

Despite these new approaches, it is noted that in the reported studies no definitive evaluations were made by comparison with the direct BP measurement. As previously reported, the auscultatory and cuff-oscillometric BP values tend to provide a significant underestimation as compared to intra-arterial BP values [18], [19]. Moreover, the reason for this difference is still unclear and remains under discussion [20]. The discrepancy is most likely to be caused by both practical and theoretical problems of these noninvasive BP measurement techniques [21], [22]. In order for the field to advance, further scientifically rigorous investigations, in which noninvasive BP measurements are compared to direct BP measurement as the gold standard, will be required in order to achieve methods with high accuracy and reliability.

IV. Electrophysiological Measurements With Dry Electrodes

There continue to be attempts to replace or complement the conventional pre-gelled electrode, used widely for research and clinical electrophysiological measurement, with so-called dry-electrodes. During the year since the previous review of "recent advances" of such electrodes [23] some further attempts of new dry electrode designs have been appeared. For example, Chi *et al.* developed a coin-sized non-contact capacitive biopotential electrode with a low-power amplifier (940 μW) and ECG measurement through clothes was successfully demonstrated [24]. Ng *et al.* developed a novel dry electroencephalography electrode with many micro-spikes of about 6 μm diameter and 110 μm length [25]. The micro-spike can penetrate the stratum corneum of the epidermidis and thereby improve electrical conductivity at the skin-electrode interface. These authors also discussed a mass production technology for the electrode employing a vacuum casting process that can allow lower-cost mass production than other methods such as the conventional electrodeposition forming or the LIGA (Lithographie, Galvanoformung, Abformung) process.

A highly interesting and noteworthy dry electrode as an alternative to the conventional gelled electrodes has been reported by Prance *et al.* [26]. They have demonstrated a new approach to electrophysiological measurement using a capacitive electrode, comprising of an ultrahigh impedance electric potential sensor. This has an input capacitance of 10 fF, and an input resistance of 10^{15} Ω. The sensor characteristics allowed the measurement of the electric field around a human body at a distance of up to 40 cm, showing that a waveform synchronized with the ECG was clearly obtained remotely from a human body *via* a 10 cm air-gap. The waveform obtained with a 40 cm air-gap was noisier than that with a 10 cm gap, but the cardiac component could still be observed. This sensor could also detect respiration signals remotely with a 40 cm air–gap. Although the waveforms obtained with this method have remained somewhat ill-defined, this completely non-contact monitoring approach could have the potential to evolve into an important new physiological measurement methdology.

V. Recent Advances in Noninvasive Optical Measurement of Blood Constituents

Noninvasive *in vivo* blood constituent measurement has a long history since the first attempts at oximetry by Millikan in 1942 [27]. Pulse oximetry invented by Aoyagi using a photoplethysmograph (PPG) with two [28] or three wavelengths [29] to measure oxygen salutation in arterial blood is undoubtedly an epoch-making example of optical measurement. Over the years, several new attempts at *in vivo* blood constituent measurement were reported. Ogawa *et al.* demonstrated a new calibration method for pulse oximetry without using the conventional ratio of absorptions, the approach being based on the use of a nonlinear regression with Support Vector Machines (SVMsR) [30]. Although the present pulse oximeter is widely used in clinical practice and many efforts have been made focusing on miniaturization, motion artifact rejection and so on, it should be noted that there still remain several practically problematic difficulties, particularly on calibration procedures. The use of SVMsR may be feasible to solve such calibration procedures.

Besides the use of the PPG for oxygen measurement as achieved with pulse oximetry, other optical techniques to measure blood constituents have been anticipated. Recently, pulse carbon monoxide oximetry, named "pulse CO-oximetry," has been proposed and substantiated in clinical use [31], [32]. It is also noted that "pulse glucometry" with a very high speed near-infrared spectrophotometer for the measurement of blood glucose, which was introduced in the previous review [23], has also now been combined with SVMsR and nonlinear classification analyses to achieve substantive results for the practical use of this method [33].

Acknowledgment

The author wishes to thank Dr. M. Ogawa for assisting in the survey of current publications relating to bioinstrumentation and Dr. P. Rolfe for his help in preparing the manuscript.

References

[1] J. W. Gordon, "Certain molar movements of the human body produced by the circulation of the blood," *J. Anat. Physiol.*, vol. 11, pt. 3, pp. 533–536, 1877.

[2] I. Starr and F. C. Wood, "Twenty-year studies with the ballistocardiograph, the relation between the amplitude of the first record of "healthy" adults and eventual mortality and morbidity from heart disease," *Circulation*, vol. 23, no. 5, pp. 714–732, 1961.

[3] K. Yamakoshi, "Unconstrained physiological monitoring in daily living for health care," *Front. Med. Biol. Eng.*, vol. 10, no. 3, pp. 239–259, 2000.

[4] K. Motoi, S. Kubota, A. Ikarashi, M. Nogawa, S. Tanaka, T. Nemoto, and K. Yamakoshi, "Development of a fully automated network system for long-term health-care monitoring at home," in *Proc. 29th IEEE EMBS Annu. Conf.*, 2007, pp. 1826–1829.

[5] O. T. Inan, M. Etemadi, R. M. Wiard, G. T. A. Kovacs, and L. Giovangrandi, "Non-invasive monitoring of valsalva-induced hemodynamic changes using a bathroom scale ballistocardiograph," in *Proc. 30th Annu. IEEE Engineering in Medicine and Biology Conf.*, 2008, pp. 674–677.

[6] O. T. Inan, M. Etemadi, A. Paloma, L. Giovangrandi, and G. T. Kovacs, "Non-invasive cardiac output trending during exercise recovery on a bathroom-scale-based ballistocardiograph," *Physiol. Meas.*, vol. 30, no. 3, pp. 261–274, Mar. 2009.

[7] O. T. Inan, M. Etemadi, R. M. Wiard, L. Giovangrandi, and G. T. Kovacs, "Robust ballistocardiogram acquisition for home monitoring," *Physiol. Meas.*, vol. 30, no. 2, pp. 169–185, Feb. 2009.

[8] D. K. Han, J. M. Kim, E. J. Cha, and T. S. Lee, "Wheelchair type biomedical system with event-recorder function," in *Proc. 30th IEEE EMBS Annu. Conf.*, 2008, pp. 1435–1438.

[9] D. K. Han, J. M. Kim, J. H. Hong, E. J. Cha, and T. S. Lee, "Performance evaluation of biosignal measurement at the wheelchair system," in *Proc. 30th IEEE EMBS Annu. Conf.*, 2008, pp. 1451–1454.

[10] D. C. Mack, J. T. Patrie, P. M. Suratt, R. A. Felder, and M. A. Alwan, "Development and preliminary validation of heart rate and breathing rate detection using a passive, ballistocardiography-based sleep monitoring system," *IEEE Trans. Inf. Technol. Biomed.*, vol. 13, no. 1, pp. 111–120, Jan. 2009.

[11] W. Chen, X. Zhu, T. Nemoto, K. Kitamura, K. Sugitani, and D. Wei, "Unconstrained monitoring of long-term heart and breath rates during sleep," *Physiol. Meas.*, vol. 29, no. 2, pp. N1–10, Feb. 2008.

[12] K. Motoi, M. Ogawa, H. Ueno, Y. Kuwae, A. Ikarashi, T. Yuji, Y. Higashi, S. Tanaka, T. Fujimoto, H. Asanoi, and K. Yamakoshi, "A fully automated health-care monitoring at home without attachment of any biological sensors and its clinical evaluation," in *Proc. 31st IEEE EMBS Annu. Conf.*, Sep. 2009, pp. 4323–4326.

[13] D. Chemla, J. L. Teboul, and C. Richard, "Noninvasive assessment of arterial pressure," *Curr. Opin. Crit. Care.*, vol. 14, no. 3, pp. 317–321, Jun. 2008.

[14] J. Muehlsteff, X. A. Aubert, and G. Morren, "Continuous cuff-less blood pressure monitoring based on the pulse arrival time approach: The impact of posture," in *Proc. 30th IEEE EMBS Annu. Conf.*, 2008, pp. 1691–1694.

[15] J. H. Shin, K. M. Lee, and K. S. Park, "Non-constrained monitoring of systolic blood pressure on a weighing scale," *Physiol. Meas.*, vol. 30, no. 7, pp. 679–693, July 2009.

[16] S. Suzuki and K. Oguri, "Cuffless and non-invasive systolic blood pressure estimation for aged class by using a photoplethysmograph," in *Proc. 30th IEEE EMBS Annu. Conf.*, 2008, pp. 1327–1330.

[17] P. A. Shaltis, A. T. Reisner, and H. H. Asada, "Cuffless blood pressure monitoring using hydrostatic pressure changes," *IEEE Trans. Biomed. Eng.*, vol. 55, no. 6, pp. 1775–1777, Jun. 2008.

[18] F. H. Van Bergen, D. S. Weatherhead, A. E. Treloar, A. B. Dobkin, and J. J. Buckley, "Comparison of indirect and direct methods of measuring arterial blood pressure," *Circulation*, vol. 10, no. 4, pp. 481–490, Oct. 1954.

[19] A. Bur, M. M. Hirschl, H. Herkner, E. Oschatz, J. Kofler, C. Woisetschlager, and A. N. Laggner, "Accuracy of oscillometric blood pressure measurement according to the relation between cuff size and upper-arm circumference in critically ill patients," *Crit. Care. Med.*, vol. 28, no. 2, pp. 371–376, Feb. 2000.

[20] J. N. Amoore, Y. Lemesre, I. C. Murray, S. Mieke, S. T. King, F. E. Smith, and A. Murray, "Automatic blood pressure measurement: The oscillometric waveform shape is a potential contributor to differences between oscillometric and auscultatory pressure measurements," *J. Hypertens.*, vol. 26, no. 1, pp. 35–43, Jan. 2008.

[21] K. Yamakoshi, , P. A. Oberg, T. Togawa, and F. Spelman, Eds., "Non-invasive cardiovascular huemodynamic measurements," in *Sensors in Medicine and Health Care*. Weinheim, Germany: Wiley-VCH Verlag, 2004, vol. 3, pp. 107–160, (Sensors Applications).

[22] K. Yamakoshi, "Volume-compensation method for non-invasive measurement of instantaneous arterial blood pressure—Principle, methodology, and some applications," *Homeostasis*, vol. 36, no. 2–3, pp. 90–119, 1995.

[23] K. Yamakoshi, "In the spotlight: BioInstrumentation," *IEEE Rev. Biomed. Eng.*, vol. 1, pp. 2–3, 2008.

[24] Y. M. Chi, S. R. Deiss, and G. Cauwenberghs, "Non-contact low power EEG/ECG electrode for high density wearable biopotential sensor networks," in *Proc. Sixth Int. Workshop on Wearable and Implantable Body Sensor Networks*, 2009, pp. 246–250.

[25] W. C. Ng, H. L. Seet, K. S. Lee, N. Ning, W. X. Tai, M. Sutedja, J. Y. H. Fuh, and X. P. Li, "Micro-spike EEG electrode and the vacuum-casting technology for mass production," *J. Materials Processing Technology*, vol. 209, no. 9, pp. 4434–4438, May 2009.

[26] R. J. Prance, S. T. Beardsmore-Rust, P. Watson, C. J. Harland, and H. Prance, "Remote detection of human electrophysiological signals using electric potential sensors," *Appl. Phys. Lett.*, vol. 93, no. 2, p. 033906, 2008.

[27] G. A. Millikan, "The oximeter, an instrument for measuring continuously the oxygen saturation of arterial blood in man," *Rev. Sci. Instrum.*, vol. 13, pp. 434–444, 1942.

[28] T. Aoyagi and K. Miyasaka, "Pulse oximetry: Its invention, contribution to medicine, and future tasks," *Anesth. Analg.*, vol. 94, no. 1, pp. S1–3, Jan. 2002, Suppl.

[29] T. Aoyagi, M. Fuse, N. Kobayashi, K. Machida, and K. Miyasaka, "Multiwavelength pulse oximetry: Theory for the future," *Anesth. Analg.*, vol. 105, no. 6, pp. S53–8, Dec. 2007, Suppl, tables of contents.

[30] M. Ogawa, Y. Yamakoshi, M. Nogawa, T. Yamakoshi, K. Motoi, S. Tanaka, and K. Yamakoshi, "A new calibration method with support vector machines for pulse oximetry," in *Proc. 4th Eur. Conf. IFMBE*, Nov. 2008, pp. 1125–1127.

[31] S. Suner and J. McMurdy, "Masimo rad-57 pulse co-oximeter for noninvasive carboxyhemoglobin measurement," *Expert Rev. Med. Devices*, vol. 6, no. 2, pp. 125–30, Mar. 2009.

[32] S. J. Barker, J. Curry, D. Redford, and S. Morgan, "Measurement of carboxyhemoglobin and methemoglobin by pulse oximetry: A human volunteer study," *Anesthesiol.*, vol. 105, no. 5, pp. 892–897, Nov. 2006.

[33] Y. Yamakoshi, M. Ogawa, and T. Tamura, "Multivariate regression and classification models for estimation of blood glucose levels using a new non-invasive optical measurement technique named "pulse-glucometry"," *The Open Optics J.*, vol. 3, pp. 63–69, Sep. 2009.

社団法人 電子情報通信学会
THE INSTITUTE OF ELECTRONICS,
INFORMATION AND COMMUNICATION ENGINEERS

信学技報
IEICE Technical Report
MBE2009-1(2009-5)

容積振動型血圧計測法の高精度化に関する研究

日下部朋哉* 野川雅道 山越健弘 田中志信 山越憲一

＊金沢大学 自然科学研究科，金沢大学 理工研究域

〒920-1192 金沢市角間町 Phone/Fax:076-234-4760

あらまし 無侵襲血圧計測法である容積振動法（間欠法）の高精度化に関して研究を行っている．今回，血管の圧-容積曲線に基づいた最高・最低血圧の決定方法を開発することにより，精度の向上を直接血圧計（Bland-Altman plot（±SD）において最高血圧誤差:2.3±7.7[mmHg],最低血圧誤差-1.8±6.4[mmHg],n=2）において確認した．本法の開発により，容積振動法の精度が向上した．

キーワード 血圧計測，容積振動法，血管圧－容積関係

Improvement of volume-oscillometric noninvasive blood pressure measurement method

Tomoya KUSAKABE*, Masamichi NOGAWA, Takehiro YAMAKOSHI, Shinobu TANAKA and Ken-ichi YAMAKOSHI

*Kanazawa University, Graduate School of Natural Science & Technology
Kanazawa University, College of Science and Engineering

Kanazawa city, Kakuma-machi, 920-1192, JAPAN

Abstract A novel intermittent noninvasive blood pressure measurement method based on vascular unloading technique has been developed to determine systolic and diastolic blood pressure (SBP, DBP) with clear physical assumption. The accuracy of the method was evaluated through the direct blood pressure measurement method. The Bland-Altman plots (±SD) of the SBP, 2.3±7.7[mmHg], and DBP, -1.8±6.4[mmHg]were obtained. The novel blood pressure measurement method has been well demonstrated with high accuracy.

Keywords: blood pressure, volume-oscilometric method, vascular-unloading technique

1． まえがき

我が国において高齢化率の上昇や不適切な生活習慣により,高血圧人口が増加傾向にある.慢性的な高血圧は動脈硬化を引き起こし,その結果,循環器系疾患となる可能性が高いことから，血圧を日常的に計測・管理し,正常な値に保つことが大切である.一般的に使用されている無侵襲間欠式血圧計測法であるカフ振動法は，平均血圧に対応するカフ内圧の振幅最大点を基準にして，その振幅の減衰比から，最高・最低血圧を決定しているが，その振幅の減衰比などの具体的な値は，経験的・統計的に決定していることから，物理的な背景が明確にされないまま使用されているのが現状である． 一方，間欠式血圧計測法である容積振動法においては，平均血圧に対応する血管容積変化（容積脈波）の振幅最大点および，消失点・出現点を最高血圧として決定出来る利点があるが[1,2]，最低血圧に関しては，いくつかの提案が行われているが，簡単には決定が困難であった[3,4].

そこで,本研究では，従来の容積振動法を再検討することで，測定原理が物理的・力学的に明確な最高・平均・最低血圧の新たな決定法を開発したので報告する.

2． 容積振動法の改良

間欠式血圧計測法である容積振動法は，図1に示す血管の力学特性である圧－容積曲線に基づいて，血管内外圧の平衡点である平均血圧に対応する血管容積 V_0 を血管容積振動（容積脈波）の振幅最大点から決定する[1,2]．ここで，図1に示すように血管容積変化(dV/dP_c)の最大点を V_0 として捕らえなおすことが可能である．この原理を最高(DBP)・最低血圧(SBP)の平衡点にも適用して考えると，図2に示す新たな血圧計測原理を提案することが可能である．本研究では，血管容積を光電容積信号として検出することから，光電的に検出する無負荷時血管容積(V_0)を PG_{V0} と表記する.

具体的には，一拍毎の脈波ボトム(PG_D)及び脈波ピーク(PG_S)とそれらに対応する外圧(P_c)を検出し,圧—容積関係に基づいたエンベロープを描き，そこで外圧に対する血管容積変化(dV/dP_c)を適用すると，血管容積変化の最大点に対応する血管容積が最低血圧(DBP)及び最高血圧(SBP)時の無負荷時血管容積であると考えられ,それぞれの血管容積を $PG_{V0\text{-}D}$ 及び $PG_{V0\text{-}S}$ と名付けることとした．理想的な血管状態を考慮すると $PG_{V0\text{-}D}$, $PG_{V0\text{-}S}$, PG_{V0} は全て一致すると考えられる．この $PG_{V0\text{-}D}$, $PG_{V0\text{-}S}$ 及び PG_{V0} のパラメータの関係から適切な血圧決定法について検討を行った.

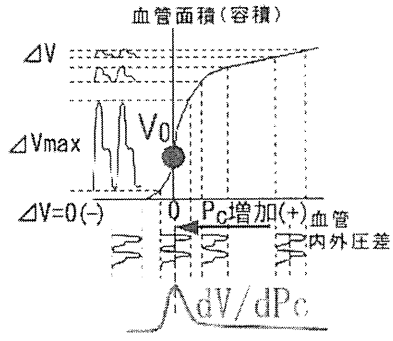

図 1　動脈の力学特性(圧—容積曲線)

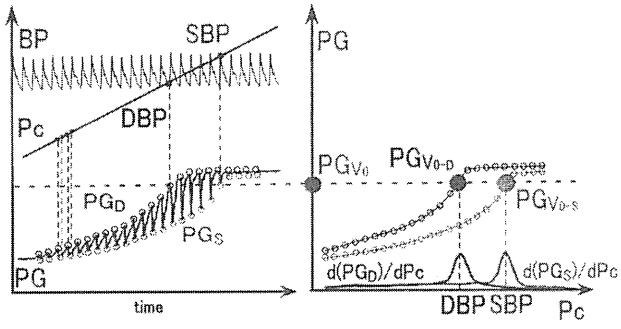

図 2　新規容積振動法の原理

3．試作無侵襲手首血圧計測システム

図 3 に本研究で用いた試作無侵襲手首血圧計測システムの概要図を示す.LED とフォトダイオード(PD)を用いた光センサにより,血管容積を光電的に検出し,光電容積(PG)やカフ圧(P_c)を DSP Board(DS1104; dSPACE GmbH,ドイツ)を介して A/D 変換を行う.Matlab/Simlink で作成したコントローラを実装した DSP から D/A 変換を行い,電空変換器(EPC)へ信号が送られ,Pc を制御することで,血管容積を制御している.手首固定具はラチェット式で,片手で装着可能である.固定具には圧力センサや EPC が一体化しており,カフ圧を瞬時に制御可能である.

4．実験方法

被験者は 2 名を対象とし,右手首に本システム,左手首に直接法を適用した.実験後の容積振動法の解析により $PG_{V0\text{-}D}$,PG_{V0}, $PG_{V0\text{-}S}$を取得した.左手首では直接血圧値を計測した.尚,本実験は金沢大学医学系倫理審査委員会の承認を経て実施した.

5．実験結果

図 4 に実験結果例を示す.図 4 の右側は外圧に対する血管容積変化 dPG/dP_c のグラフで,それぞれのピークに対応するカフ圧は,SBP が 122mmHg, DBP が 78mmHg であった.また,容積振動法中の直接血圧値 BP は SBP が 128mmHg, DBP が 77mmHg であり, 容積振動法における SBP 及び DBP が良好に計測できた.同時に取得した $PG_{V0\text{-}D}$, V_0 及び $PG_{V0\text{-}S}$は $PG_{V0\text{-}D} \leqq V_0 \leqq PG_{V0\text{-}S}$の関係を満たしていた.

図 5 は直接法と容積振動法から取得した SBP 及び DB と直接血圧値を評価した結果である.全データから, $PG_{V0\text{-}D}$,PG_{V0}及び $PG_{V0\text{-}S}$が $PG_{V0\text{-}D} \leqq PG_{V0} \leqq PG_{V0\text{-}S}$の関係を満たすデータを抽出すると, Bland-Altman plot において,DBP に関しては平均誤差±SD=-1.8±6.4[mmHg], SBP に関しては平均誤差±SD=2.3±7.7[mmHg]であり,直接法と比較して最も良好な値を取得できた.即ち容積振動法において $PG_{V0\text{-}D}$,PG_{V0} 及び $PG_{V0\text{-}S}$ が $PG_{V0\text{-}D} \leqq PG_{V0} \leqq PG_{V0\text{-}S}$の関係を満たす時, 適切な PG_{V0}を計測出来ると考えられる.$PG_{V0\text{-}D}$,PG_{V0}及び $PG_{V0\text{-}S}$が全て一致しないのは,血管壁の粘性に由来するヒステリシスに起因するものと考えられる.

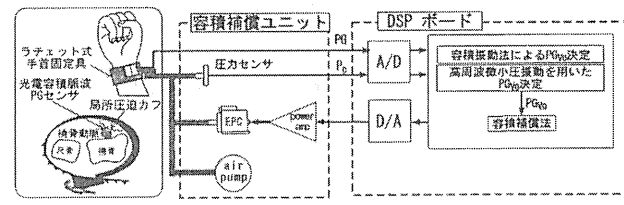

図 3　試作手首血圧計測システム概要図

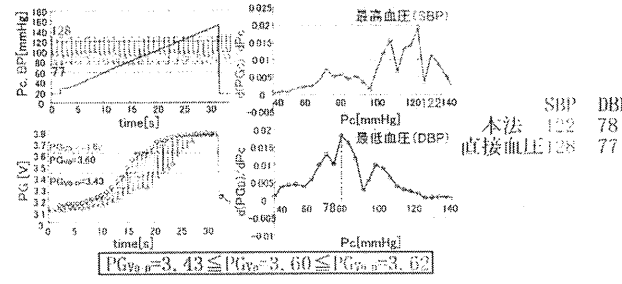

図 4　手首容積振動法計測結果例

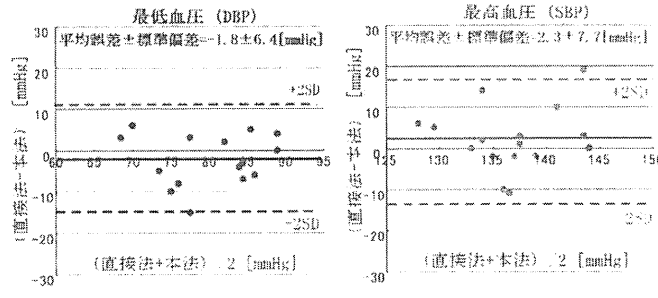

図 5　Bland-Altman plot による手首容積振動法の DBP,SBP と直接血圧値の評価

6. 結言

本研究では,容積振動法の改良法を提案し，容積振動法実施時に取得した圧力変化に対する血管容積変化の 3 種類の最大点 $PG_{V0\text{-}D}$, PG_{V0} 及び $PG_{V0\text{-}S}$ が $PG_{V0\text{-}D} \leqq PG_{V0} \leqq PG_{V0\text{-}S}$ の関係を満たす時に,DBP 及び SBP は直接血圧値と良好に一致することを確認した.

参考文献

[1] Yamakoshi K, Shimazu H, Shibata M, Kamiya A., New oscillometric method for indirect measurement of systolic and mean arterial pressure in the human finger. Part 1: model experiment., Med Biol Eng Comput. May;20(3):307-13, 1982

[2] Yamakoshi K, Shimazu H, Shibata M, Kamiya A., New oscillometric method for indirect measurement of systolic and mean arterial pressure in the human finger. Part 2: correlation study., Med Biol Eng Comput. May;20(3):314-8, 1982

[3] Shimazu H, Ito H, Kobayashi H, Yamakoshi K., Idea to measure diastolic arterial pressure by volume oscillometric method in human fingers., Med Biol Eng Comput. Sep;24(5):549-54, 1986

[4] Shimazu H, Ito H, Kawarada A, Kobayashi H, Hiraiwa A, Yamakoshi K., Vibration technique for indirect measurement of diastolic arterial pressure in human fingers., Med Biol Eng Comput. Mar;27(2):130-6., 1989

Journal of Molecular and Cellular Cardiology 48 (2010) 680–693

Contents lists available at ScienceDirect

Journal of Molecular and Cellular Cardiology

journal homepage: www.elsevier.com/locate/yjmcc

Original article

Donepezil, an acetylcholinesterase inhibitor against Alzheimer's dementia, promotes angiogenesis in an ischemic hindlimb model

Yoshihiko Kakinuma [a,*], Mutsuo Furihata [b], Tsuyoshi Akiyama [c], Mikihiko Arikawa [a], Takemi Handa [a], Rajesh G. Katare [a], Takayuki Sato [a]

[a] Department of Cardiovascular Control, Kochi Medical School, Nankoku, Kochi 783-8505, Japan
[b] Department of Pathology, Kochi Medical School, Nankoku, Japan
[c] Department of Cardiac Physiology, National Cardiovascular Center Research Institute, Suita, Japan

ARTICLE INFO

Article history:
Received 12 May 2009
Received in revised form 7 November 2009
Accepted 10 November 2009
Available online 3 December 2009

Keywords:
Angiogenesis
Vascular endothelial growth factor
Acetylcholinesterase inhibitor
Donepezil

ABSTRACT

Our recent studies have indicated that acetylcholine (ACh) protects cardiomyocytes from prolonged hypoxia through activation of the PI3K/Akt/HIF-1α/VEGF pathway and that cardiomyocyte-derived VEGF promotes angiogenesis in a paracrine fashion. These results suggest that a cholinergic system plays a role in modulating angiogenesis. Therefore, we assessed the hypothesis that the cholinergic modulator donepezil, an acetylcholinesterase inhibitor utilized in Alzheimer's disease, exhibits beneficial effects, especially on the acceleration of angiogenesis. We evaluated the effects of donepezil on angiogenic properties *in vitro* and *in vivo*, using an ischemic hindlimb model of α7 nicotinic receptor-deleted mice (α7 KO) and wild-type mice (WT). Donepezil activated angiogenic signals, i.e., HIF-1α and VEGF expression, and accelerated tube formation in human umbilical vein endothelial cells (HUVECs). ACh and nicotine upregulated signal transduction with acceleration of tube formation, suggesting that donepezil promotes a common angiogenesis pathway. Moreover, donepezil-treated WT exhibited rich capillaries with enhanced VEGF and PCNA endothelial expression, recovery from impaired tissue perfusion, prevention of ischemia-induced muscular atrophy with sustained surface skin temperature in the limb, and inhibition of apoptosis independent of the α7 receptor. Donepezil exerted comparably more effects in α7 KO in terms of angiogenesis, tissue perfusion, biochemical markers, and surface skin temperature. Donepezil concomitantly elevated VEGF expression in intracardiac endothelial cells of WT and α7 KO and further increased choline acetyltransferase (ChAT) protein expression, which is critical for ACh synthesis in endothelial cells. The present study concludes that donepezil can act as a therapeutic tool to accelerate angiogenesis in cardiovascular disease patients.

1. Introduction

Studies investigating the effects of vagal nerve stimulation (VS) on heart failure have suggested VS as a candidate for a therapeutic modality in heart failure because VS suppresses infarction-induced fatal arrhythmia and progression of ventricular remodeling [1,2]. However, the precise mechanisms remain to be fully elucidated.

To further investigate the underlying mechanisms of the VS effects, we have focused on disclosing the pleiotropic effects of acetylcholine (ACh) and revealed that ACh prevents cardiomyocytes from persistent hypoxia-induced cell death and have ultimately presented a new concept regarding ACh as a trophic factor. Our recent study demonstrated that ACh directly transduces cell survival signal through the muscarinic receptor, activates the PI3K/Akt/HIF-1α/VEGF pathway, inhibits collapse of mitochondrial membrane potential, and inactivates caspase-3 in cardiomyocytes subjected to hypoxia [3]. Because both survival and angiogenic pathways share common signaling molecules through HIF-1α/VEGF, these results prompted us to speculate the involvement of ACh in modulation of angiogenesis.

Furthermore, ACh transduces signals through nitric oxide (NO) production, and NO plays a key role in angiogenesis [4–8]. Specifically, according to our previous study, the NO donor *S*-nitroso-*N*-acetylpenicillamine activates the PI3K/Akt/HIF-1α pathway to increase VEGF expression in cardiomyocytes, and VEGF derived from cardiomyocytes accelerates tube formation in human umbilical endothelial cells (HUVECs), i.e., *in vitro* angiogenesis [4].

In contrast to these positive results, few *in vivo* studies have demonstrated the effects of systemically administered ACh because of its severe side effects including induction of bronchospasm and airway mucus hypersecretion. To circumvent this, we used donepezil, an acetylcholinesterase inhibitor and anti-Alzheimer's drug, that

* Corresponding author. Tel.: +81 88 880 2587; fax: +81 88 880 2310.
E-mail address: kakinuma@kochi-u.ac.jp (Y. Kakinuma).

0022-2828/$ – see front matter © 2009 Elsevier Ltd. All rights reserved.
doi:10.1016/j.yjmcc.2009.11.010

elevates local levels of ACh without such adverse effects [9,10]. In addition, we tested the effect of donepezil in a murine hindlimb ischemia model. To extensively investigate the effect of donepezil, we used α7 nicotinic receptor-deleted mice (α7 KO) suffering from impaired angiogenesis with characteristic mechanisms [11-13]. In the present study, we demonstrated a novel effect of donepezil on angiogenesis, i.e., acceleration of angiogenesis.

2. Materials and methods

2.1. Murine hindlimb ischemia model and donepezil administration

Male C57BL6/J mice (WT) ($n=45$) and α7 KO ($n=26$) aged 10–12 weeks were used. After anesthesia with pentobarbital sodium (30 mg/kg), the left femoral artery was completely ligated at its

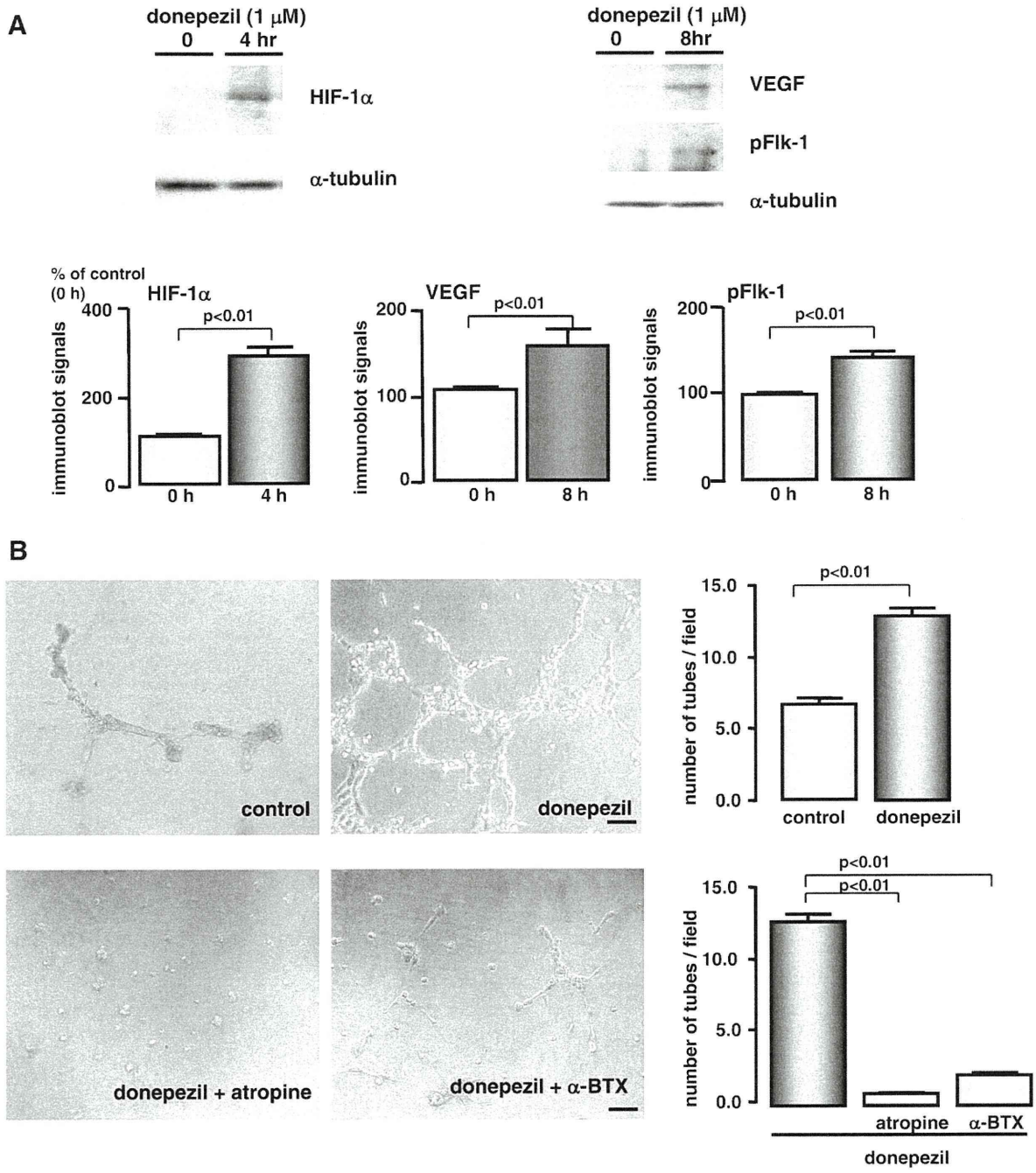

Fig. 1. Donepezil mediates angiogenic signals in HUVECs to activate tube formation. (A) Donepezil (1 μM) increased the HIF-1α protein expression level during normoxic conditions. This induction of HIF-1α was followed by increased VEGF expression and activated phosphorylation of the VEGF type 2 receptor Flk-1 in HUVECs ($n=3$). (B) Donepezil also accelerated tube formation in HUVECs (12.8 ± 0.6 tube number per field vs. 6.7 ± 0.4 in control, $P<0.01$, $n=3$). In contrast, donepezil-induced tube formation was inhibited by atropine (100 μM) or α-bungarotoxin (0.1 μM). Scale bar represents 50 μm. Representative data from 3 experiments are shown for each study. (C) ACh (100 μM) and nicotine (0.1 μM) increased HIF-1α and VEGF protein expression. (D) Tube formation in untreated HUVECs progressed within 24 h, and ACh markedly accelerated tube formation. ACh (100 μM) accelerated tube formation (16.8 ± 0.9 in 100 μM of ACh vs. 7.3 ± 0.5, $P<0.01$, $n=3$). ACh-induced acceleration of tube formation was partly suppressed by atropine (100 μM) (2.8 ± 0.8, $P<0.01$, $n=3$) and α-bungarotoxin (0.1 μM) (2.7 ± 0.6, $P<0.01$, $n=3$). Scale bars represent 100 μm. Representative data from 3 experiments are shown for each study (D).

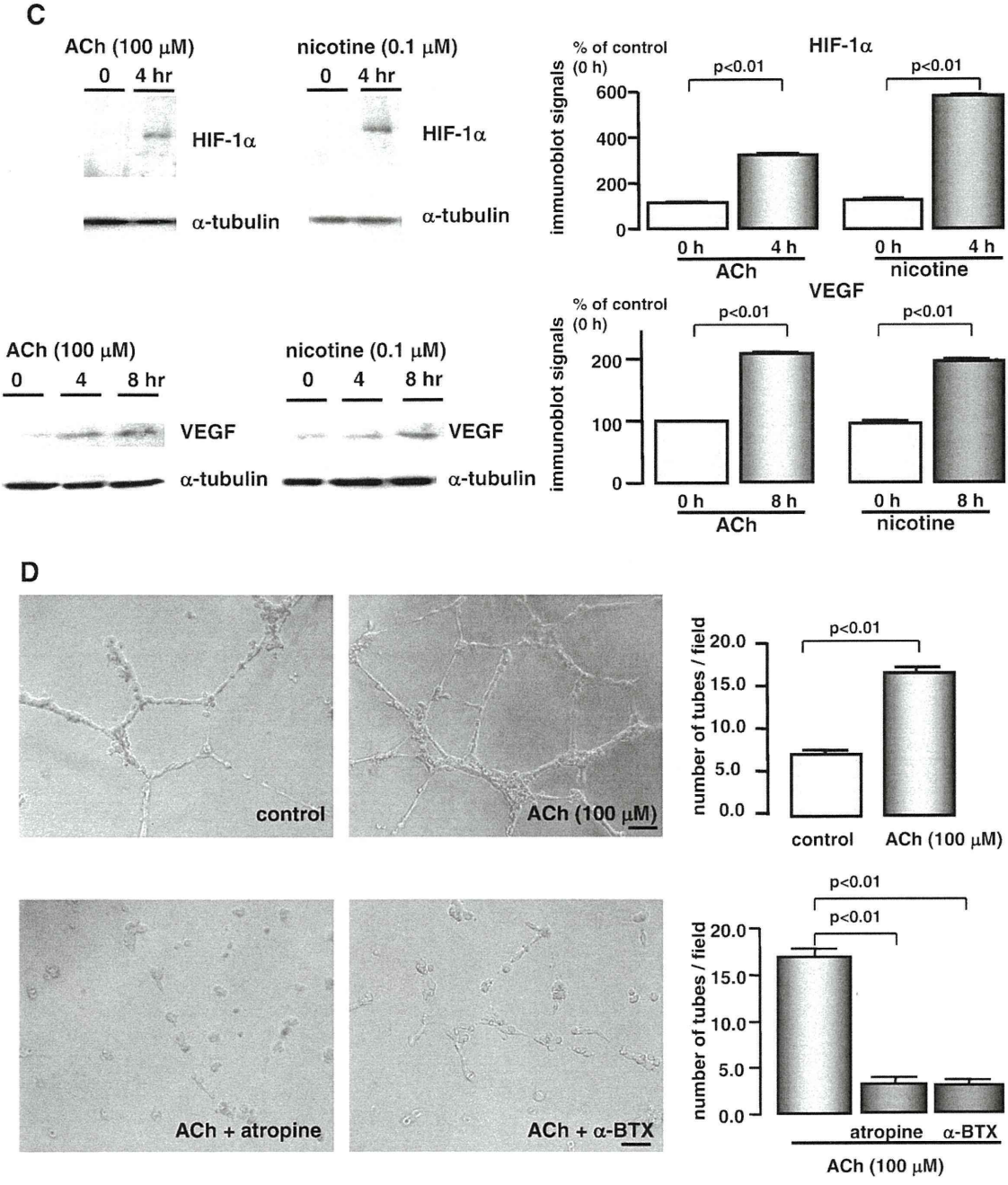

Fig. 1 (*continued*).

proximal end. Ligation was verified to be successful by pallor of the left foot. Donepezil (5 mg/kg/day) dissolved in drinking water (50 mg/L) was orally administered *ad lib* for 4 weeks. This dose was initially determined to clearly show the expected effects without producing adverse effects in the mice.

To investigate the involvement of cholinergic receptors on the effects of donepezil in terms of angiogenesis *in vivo* and to compare it with WT treated with donepezil alone, further donepezil-treated WT were divided into 3 subgroups ($n=6$–9 in each group) receiving one of the following treatments for 4 weeks: (a) α-bungarotoxin (14 μg/kg/day by i.m. on the flank), (b) mecamylamine (2.1 mg/kg/day i.m. on the flank), and (c) atropine (5 mg/kg/day p.o.) [14]. Another experimental study was conducted on α7 KO with a lower dose (0.083 mg/kg/day) using the same experimental schedule ($n=9$). This lower dose was comparable with that prescribed for patients. At the end of the treatment period, the heart and quadriceps femoris muscle were excised for experiments. Our preliminary study verified that even higher dose of donepezil, 5 mg/kg/day, does not down-regulate heart rate or blood pressure.

2.2. Angiography using indocyanine green dye

To functionally evaluate the effects of donepezil on murine angiogenesis, angiography was performed using indocyanine green (ICG) (Sigma-Aldrich, St. Louis, MO, USA), which clearly visualize tissue perfusion in the hindlimb. After anesthesia with pentobarbital sodium, both lower extremities were shaved. The field was illuminated by an LED-fluorescence imaging device, and ICG was admin-

istered intravenously (0.3 mg/kg). After a bolus ICG injection, real-time imaging analysis was performed using an infrared camera and recorded with a digital camcorder for an optimized time. Our preliminary studies identified that ICG angiography in the hindlimbs initially revealed an angiogram, followed by a perfusion phase, when the fluorescence signals in the perfused tissue were simultaneously and homogeneously increased in both hindlimbs. After recording, the fluorescence intensity in the hindlimb was evaluated. Therefore, to evaluate perfusion in an ischemic hindlimb, the interested regions were selected from both right and left hindlimbs. The fluorescence signals of the left hindlimb in the perfusion phase were compared with those of the right, using NIH image software, and it revealed laterality in the ICG signal intensity. The time when the signal difference between the right and left was extremely evident was selected.

2.3. Evaluation of the relative blood flow using fluorescent microspheres

According to previous studies using fluorescent microspheres [15,16], we evaluated the relative blood flow between the left and right hindlimbs in mice. Briefly, after anesthesia, 200 μL of green FluoSphere fluorescent microspheres (15 μm, Molecular Probes, Invitrogen, Carlsbad, CA, USA) was administered within 1 min, followed by immediate sampling of blood and bilateral quadriceps femoris muscles. These samples were weighed accurately and incubated in 4 M KOH containing 2% of Tween 80 at 70 °C for 24 h. After measuring the fluorescence, the ratio of the fluorescence between the left and right hindlimbs, corrected by the tissue weight, was compared.

2.4. Thermography

One day after surgery, an initial temperature evaluation was performed in the hindlimbs using infrared thermography (MobIR M4 Thermal Camera, Wuhan Guide Infrared Technology Co., Ltd. China). The skin temperature of the mice under anesthesia was measured 3 times. Thereafter, for each mouse, temperature was evaluated 3 times by thermography during 4 weeks. The temperature distribution in the hindlimbs was compared between donepezil-treated and untreated mice and standardized by each non-ligated hindlimb as a reference. The laterality in temperature, represented by the ratio between the left and right hindlimb temperature, was evaluated.

2.5. Immunohistochemistry

The heart and quadriceps femoris muscle were excised and fixed in 4% paraformaldehyde. Some muscle samples were routinely

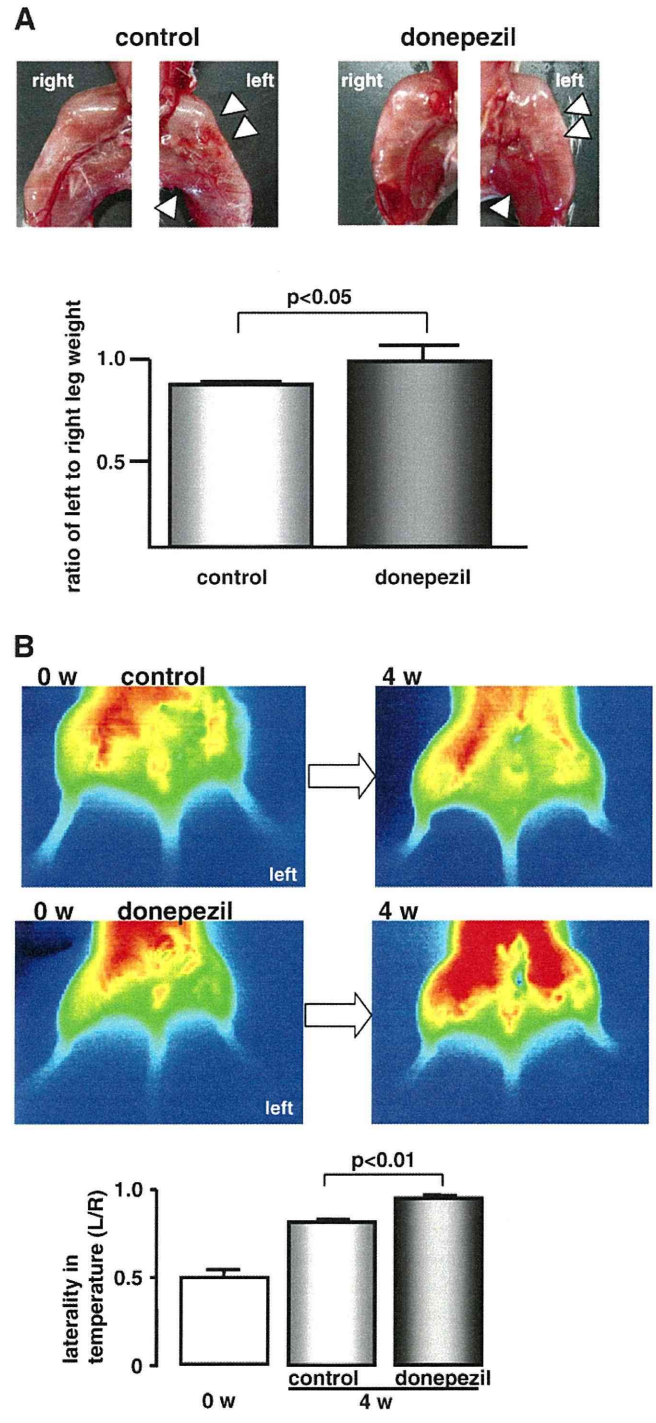

Fig. 2. Donepezil promotes angiogenesis in C57 BL6/J wild-type mice (WT) suffering from left hindlimb ischemia and suppresses ischemia-induced muscular atrophy and reduction of skin temperature. (A) WT treated with orally administered donepezil showed comparable muscular volume between the right and left hindlimb, even with the left hindlimb ischemia (arrowheads in the right panel), compared with untreated WT mice (arrowheads in the left panel) ($n=10$). (B) Donepezil accelerated skin temperature recovery in the left hindlimb within 4 weeks and sustained the skin temperature comparably to the right hindlimb. The ratio of skin temperature in the left hindlimb to the right, the laterality in the temperature, was increased by donepezil from 0.50 ± 0.04 after ligation to 0.95 ± 0.01 (vs. 0.81 ± 0.01 in control, $P<0.01$, $n=10$). (C) Compatible with this, donepezil-treated WT mice demonstrated more nuclei aligned with a vasculature-like appearance, especially in the left ischemic hindlimb (the right panel in donepezil, Fig. 2C). Magnification: ×200. Numbers of nuclei per visual field in the donepezil-treated left ischemic hindlimb increased significantly compared to the non-treated hindlimb ($P<0.01$, $n=9$). VEGF immunoreactivity was upregulated by donepezil in the left ischemic hindlimb (the right panel in Fig. 2C) compared with the control. Scale bars represent 50 μm. HIF-1α and VEGF protein expression in the left quadriceps femoris muscle increased significantly in donepezil-treated WT ($P<0.01$, $n=9$). (D) This effect of donepezil on VEGF signals did not significantly decrease following α-bungarotoxin, mecamylamine, or atropine treatment. Inhibition of caspase-3 by donepezil was also not attenuated by cholinergic antagonists. The PCNA expression level was elevated by donepezil but not reduced by α-bungarotoxin. (E) Donepezil increased VEGF and PCNA immunoreactivity, specifically in endothelial cells, whereas α-bungarotoxin did not affect VEGF- and PCNA-positive endothelial cells, as shown in the Western blot analysis. (F) Sustained skin temperature by donepezil was not blunted by α-bungarotoxin, mecamylamine, or atropine ($P<0.01$ vs. control, respectively). (G) ICG angiography revealed comparable tissue perfusion between the right and left hindlimbs in donepezil-treated WT (1.00 ± 0.84 vs. 1.08 ± 6.1; not significant, NS, $n=3$) (arrowheads in the right panel). In contrast, untreated WT mice showed lower tissue perfusion in the left hindlimb (0.74 ± 0.27 vs. 1.00 ± 0.43, $P<0.01$, $n=3$) (arrowheads in the left panel). Representative ICG angiography data from 3 experiments are presented. A microsphere assay also showed increased blood flow in donepezil-treated hindlimbs, evaluated with the ratio of left to right fluorescent signals (115.4 ± 19.3 in donepezil vs. 75.2 ± 7.5 in control, $P<0.05$, $n=5$).

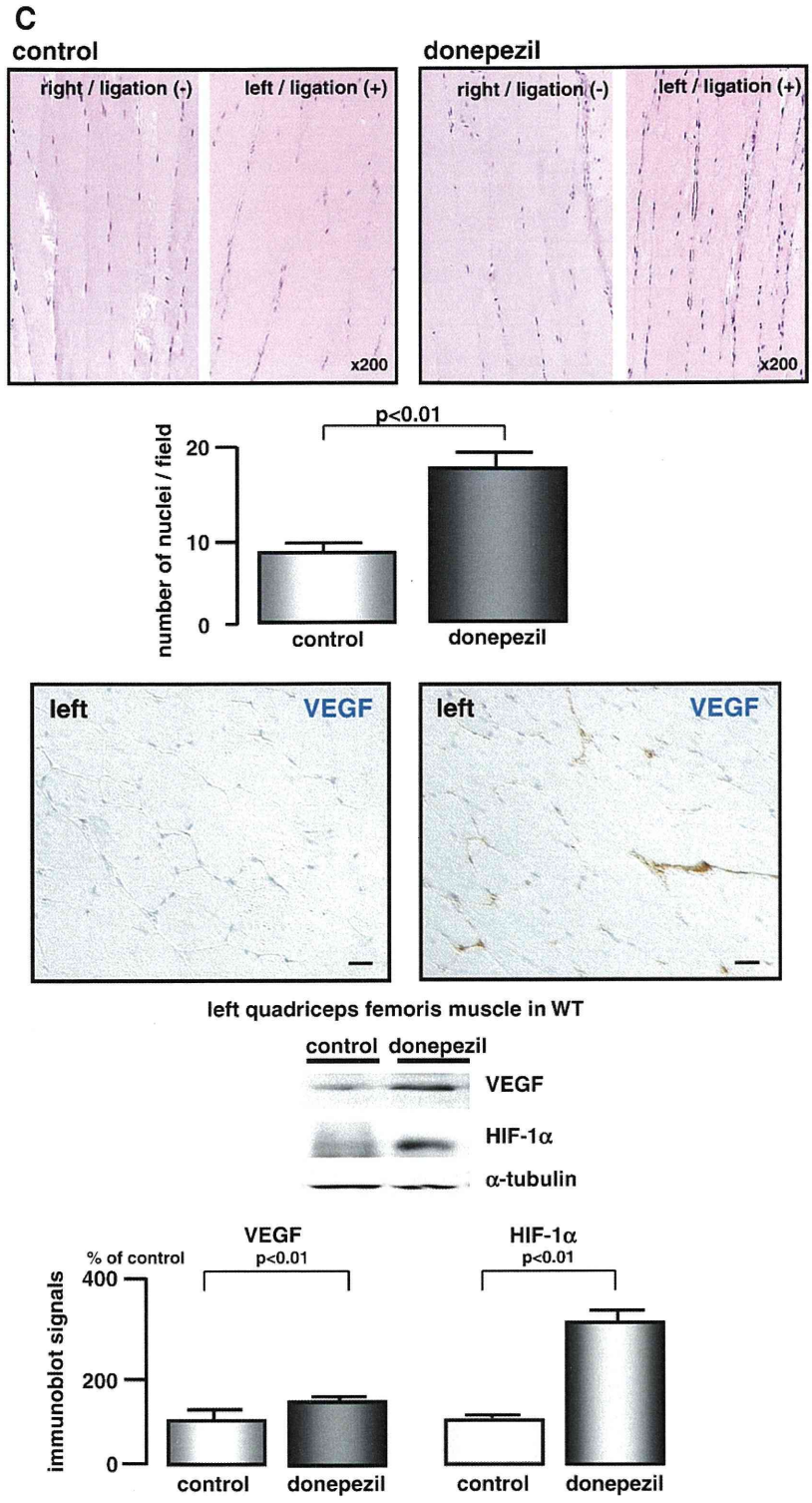

Fig. 2 (*continued*).

processed, paraffin-embedded, cut into 4-μm sections, and stained with hematoxylin and eosin. The number of nuclei in capillary-like structures per HPF were counted in randomly selected fields (9 fields per section). Other samples were used for immunohistochemical study using the Ventana automated immunohistochemistry system (Discovery TM, Ventana Medical System, Inc., Tucson, AZ, USA). Antigen retrieval was performed for 60 min in a preheated Dako Target Retrieval Solution (pH 6.0) using a microwave, followed by inhibition of intrinsic peroxidase, blocking, and the reaction with a primary antibody. VEGF and PCNA immunoreactivities were identified using a polyclonal anti-VEGF antibody at 1:100 (sc-152) (Santa Cruz Biotechnology, CA, USA) and a monoclonal anti-PCNA antibody at 1:2000 (Abcam Inc., Cambridge, MA, USA), respectively, based on the streptavidin–biotin–peroxidase reaction.

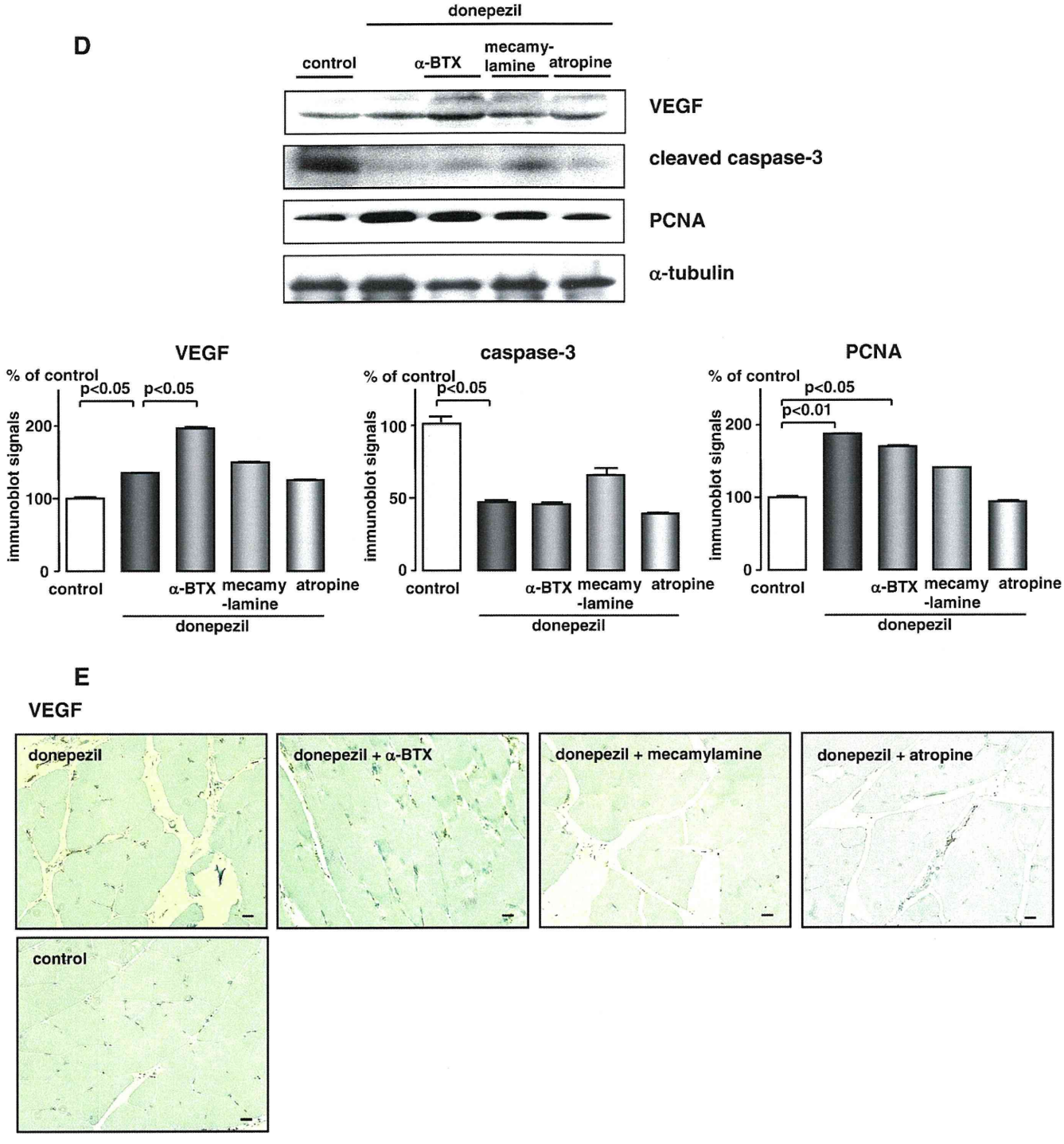

Fig. 2 (*continued*).

2.6. Western blotting

Whole muscle cell lysates were fractionated by SDS–PAGE and transferred onto membranes (Millipore Corp., Bedford, MA, USA). The membranes were incubated with polyclonal antibodies against VEGF (Santa Cruz Biotechnology), cleaved caspase-3 (Cell Signaling Technology, Danvers, MA, USA), diluted at 1:500, or with monoclonal antibodies against HIF-1α (Novus Biologicals, Inc., Littleton, CO, USA), pFlk-1 (Tyr 951, Santa Cruz Biochemistry), diluted at 1:500, α-tubulin (LAB VISION, Fremont, CA, USA), and PCNA (Abcam Inc.) diluted at 1:2000. Human umbilical vein endothelial cells (HUVECs), cultured in supplemented EGM-2 culture medium (Cambrex, Walkersville, MD, USA) on 24-well plates, were harvested with sample buffers. Similarly, the blotted membranes were incubated with a polyclonal anti-ChAT antibody (Millipore Corp., Bedford, MA, USA) diluted at 1:500, which detects several bands with an M.W. of 68–70 kDa. Each antibody was used in conjunction with a horseradish peroxidase-conjugated secondary antibody. For *in vitro* studies, each experiment was independently performed 3 times. After that, the densitometry analysis was performed.

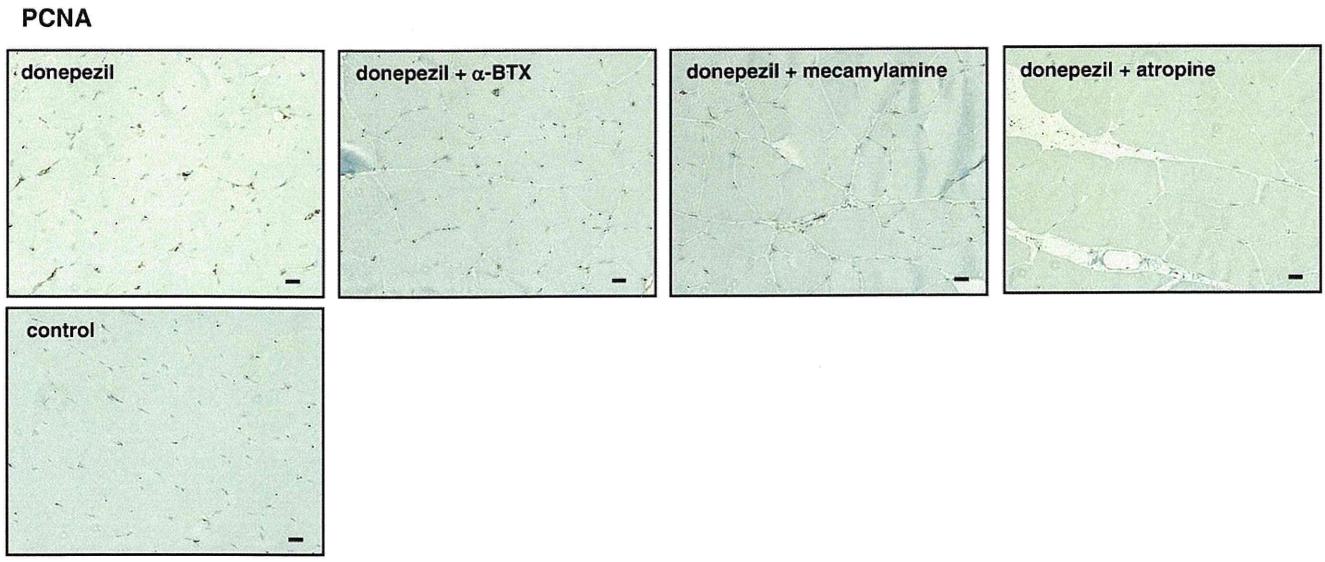

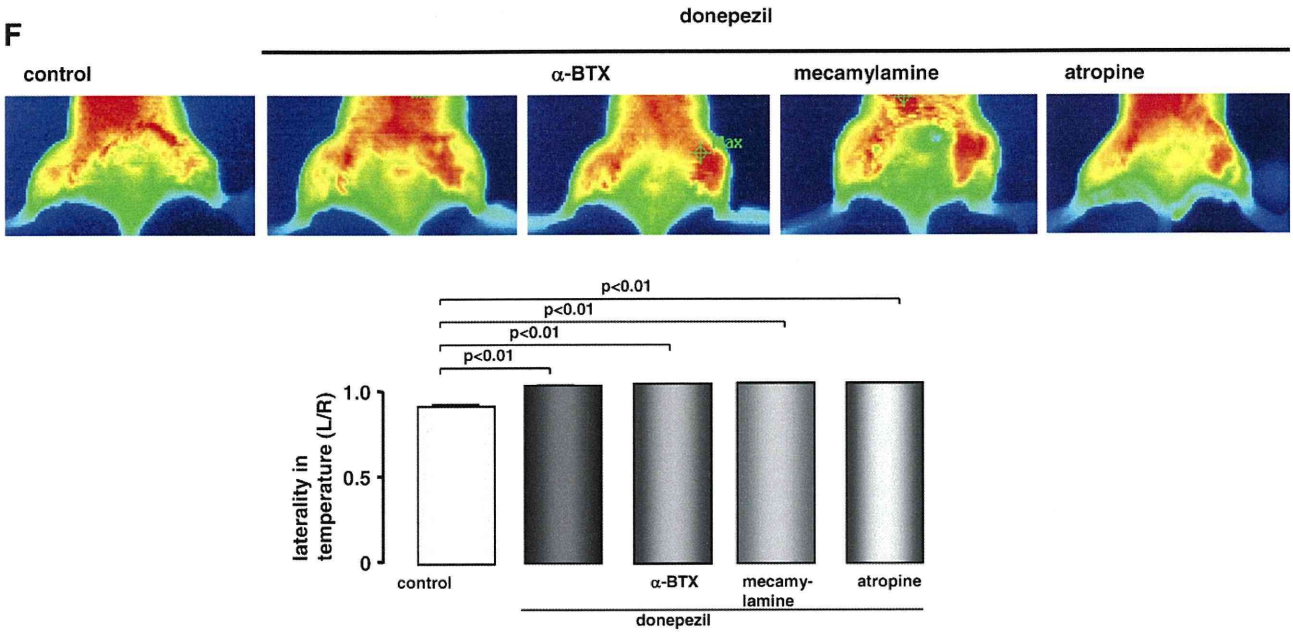

Fig. 2 (*continued*).

2.7. Reverse transcription-polymerase chain reaction (RT-PCR)

Total RNA was extracted from cells, and total RNA (1 μg) was reverse-transcribed to obtain single-stranded cDNA using a kit. Specific human cholinergic receptor primers were designed according to previous studies [17,18]. PCR amplification was performed with 40 cycles of the reaction and annealing temperatures of 60 °C. Primer sequences were as follows:

m1, TGAGGGCTCACCAGAGACT (forward),
GTCCAGGTGAGGATGAAGG (reverse);
m2, ACAAGGAAGGATAGTGAAGCC (forward),
CATCTCCATTCTGACCTGAAG (reverse);
α4, CTCACCGTCCTTCTGTGTC (forward),
CTGGCTTTCTCAGCTTCCAG (reverse);
α7, AGGCCACCTCATCAGCAG (forward),
GTACGCTGGTTTCCCTTTGA (reverse);
GAPDH, CGTCTTCACCACCATGGAGA (forward),
CGGCCATCACGCCACAGCTT (reverse).

2.8. Cell culture

HUVECs or human aorta endothelial cells (HAECs) were cultured in EGM-2 culture medium (Cambrex), supplemented with heparin, IGF-I, VEGF, bFGF, EGF, hydrocortisone, FBS, and ascorbic acid, according to the manufacturer's instruction. The final concentration of each reagent was as follows: 1 μM of donepezil (Eisai Co., Ltd., Tokyo, Japan), 0.1 μM of nicotine, which has been reported to possess angiogenic property [11-13], and 100 μM of ACh (Sigma-Aldrich, St. Louis, MO, USA).

To investigate the effects on tube formation, *in vitro* angiogenesis, HUVECs were cultured on Matrigel with complete growth factors (Becton Dickinson Labware, Bedford, MA, USA) using 96-well plates. HUVECs (1×10^4 cells) were seeded on Matrigel (50%)-coated wells

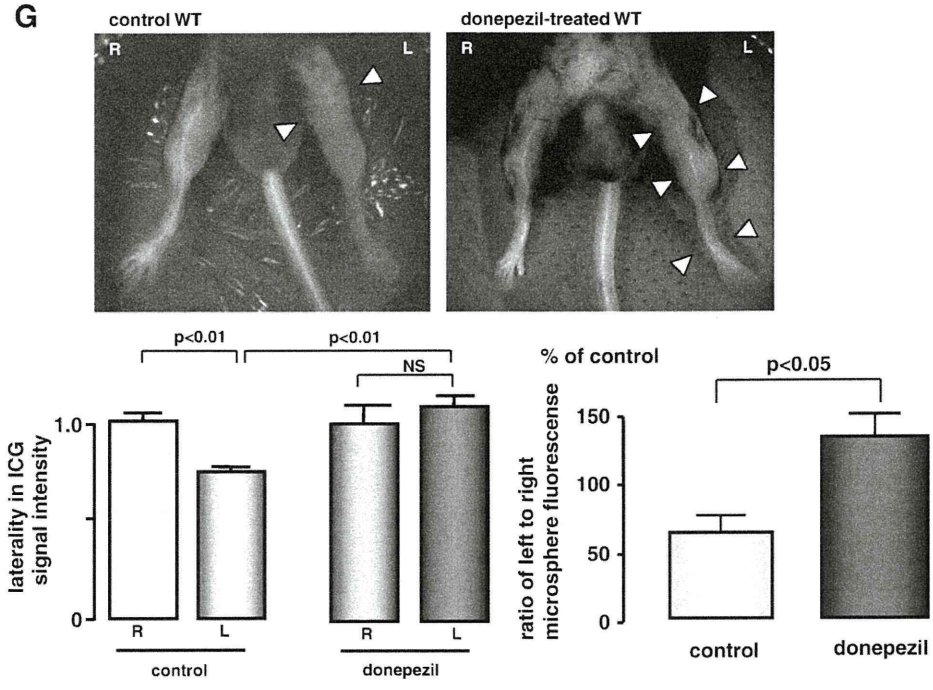

Fig. 2 (*continued*).

and incubated for 24 h in DMEM with 20% FBS, 25 μg/ml endothelial cell growth supplement (Upstate, Lake Placid, NY, USA), 10 U/ml heparin, and any one of the study agents. The number of tubes per low power field in each well was counted and compared.

2.9. MTT activity

To evaluate HUVEC proliferation, we measured the reduction activity of 3-(4,5-dimethylthiazol-2-yl)-2,5-diphenyl tetrazolium bromide (MTT). One hour before sampling, MTT reagents (10 μL) were added to the culture medium (100 μL), incubated, and the absorbance at 450 nm was measured (Cell Counting Kit-8; Dojindo, Kumamoto, Japan), according to the manufacturer's protocol.

2.10. Caspase 3/7 activity

According to the manufacturer's protocol (Promega, Madison, WI, USA), HUVECs treated with or without donepezil were cultured with an equal volume of Caspase-Glo 3/7 reagent for 3 h, followed by measuring the luminescence of each sample using the luminometer manufacturer's protocol.

2.11. Statistical analysis

The data are presented as means ± SE. The mean values between the 2 groups were compared using the unpaired Student's *t*-test. Differences among data for the in vitro studies were assessed by the Kruskal–Wallis test for multiple comparisons, followed by Scheffe's post-hoc test. Differences were considered significant at $P<0.05$.

3. Results

3.1. Donepezil activates angiogenic signals and accelerates tube formation in vitro

Donepezil transduces angiogenic signals. In the normoxic condition, donepezil (1 μM) elevated the HIF-1α protein level and then augmented expression of VEGF and activated phosphorylation of Flk-1, VEGF type 2 receptor (Fig. 1A), which composes critical angiogenic signaling. Correspondingly, donepezil enhanced tube formation (Fig. 1B) in HUVECs within 24 h (12.8 ± 0.6 in donepezil-treated HUVECs vs. 6.7 ± 0.4 in control, $P<0.01$), suggesting that donepezil is

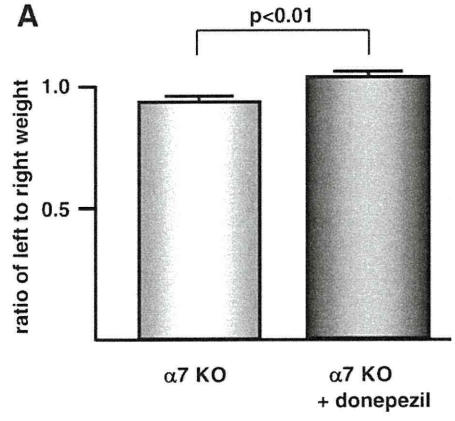

Fig. 3. Donepezil exhibits comparable angiogenic effects in the ischemic hindlimb model using α7 KO mice. (A) Donepezil inhibited ischemia-induced muscular atrophy in α7 KO. The ratio of the left leg weight to the right leg weight in donepezil-treated mice increased compared with untreated mice ($n=13$). (B) ICG angiography showed that donepezil attenuated ischemia-induced impairment of tissue perfusion (1.23 ± 0.10 vs. 0.70 ± 0.27, $P<0.01$, $n=3$) compared to untreated α7 KO. Representative ICG angiography data from 3 experiments are presented. Using a microsphere assay, donepezil inhibited the reduction of blood flow (117.4 ± 9.7 vs. 70.4 ± 10.7 in control, $P<0.05$, $n=5$ in each). (C) VEGF protein expression in the left ischemic hindlimb of donepezil-treated α7 KO increased compared with untreated α7 KO ($P<0.01$, $n=11$). More intense VEGF immunoreactivity was detected in donepezil-treated α7 KO, especially between each muscle fiber. Scale bar represents 50 μm. (D) Recovery of skin temperature in the left ischemic hindlimb of donepezil-treated α7 KO was more accelerated during the treatment (arrowheads in the lower panel). The laterality in temperature in α7 KO (0.71 ± 0.03), which was lower than that in WT (0.81 ± 0.02), increased with donepezil (0.98 ± 0.02, $P<0.01$, $n=13$). In contrast, untreated α7 KO showed poor skin temperature recovery (arrowheads in the upper panel). (E) Donepezil, even at a lower dose, inhibited the reduction in skin temperature in the left ischemic hindlimb (arrowheads in the lower panel), as evidenced by the elevation of laterality in temperature (0.96 ± 0.04, $P<0.01$, $n=9$).

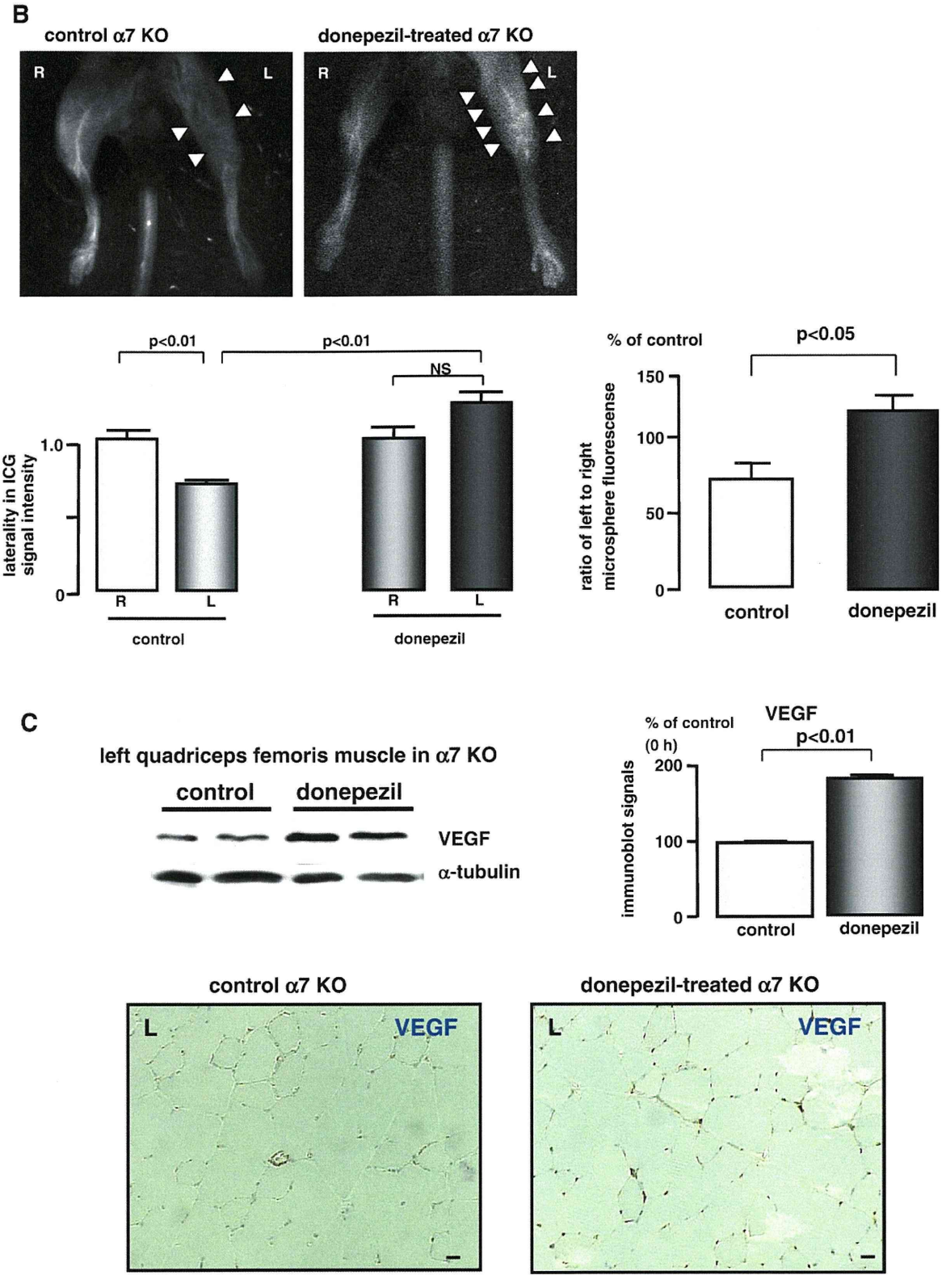

Fig. 3 (*continued*).

capable of accelerating angiogenesis. This effect of donepezil was inhibited by the muscarinic receptor antagonist atropine (100 μM) (0.7 ± 0.2, $P<0.01$) and the selective α7 nicotinic receptor antagonist α-bungarotoxin (0.1 μM) (2.0 ± 0.6, $P<0.01$) (Fig. 1B).

The mechanisms of donepezil-induced acceleration of angiogenesis were revealed by the effect of ACh as well as nicotine, which has been reported to promote angiogenesis [11-13], on HUVECs. ACh and nicotine shared the same angiogenic signals (Fig. 1C). Moreover, ACh

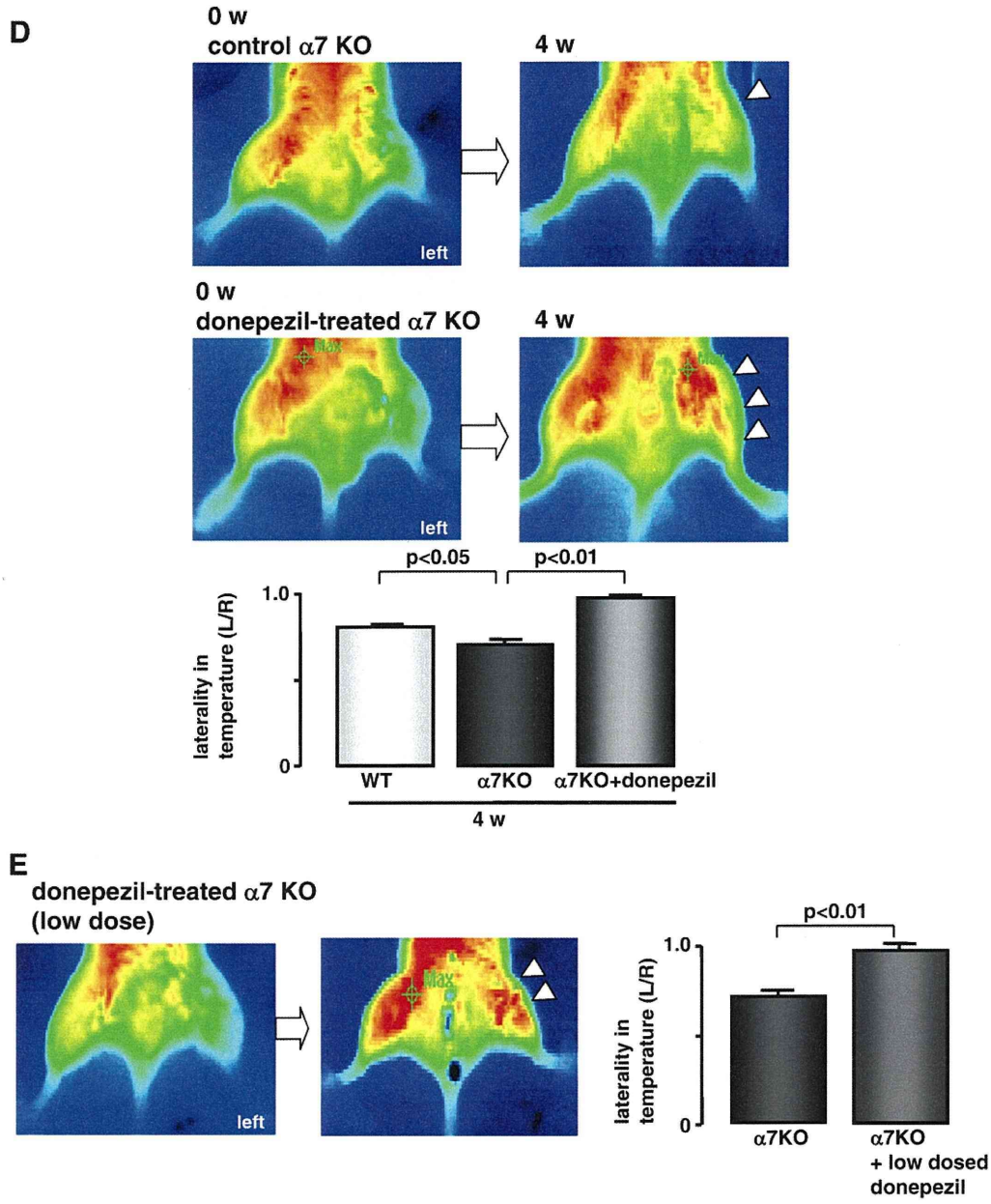

Fig. 3 (*continued*).

accelerated HUVEC tube formation within 24 h (16.8 ± 0.9 with 100 μM of ACh vs. 7.3 ± 0.5 control, $P<0.01$) (Fig. 1D); however, it was markedly suppressed by atropine (100 μM) (2.8 ± 0.8, $P<0.01$) and α-bungarotoxin (0.1 μM) (2.7 ± 0.6, $P<0.01$) (Fig. 1D). Similarly, ACh accelerated tube formation in HAECs, which was partially suppressed by atropine (data not shown). These results suggest that ACh promotes *in vitro* angiogenesis through angiogenic signal transduction and that the signal is mediated via both nicotinic and muscarinic receptors.

3.2. Donepezil promotes angiogenesis and suppresses ischemia-induced muscular atrophy in a murine hindlimb ischemia model

In untreated WT, muscular atrophy of the left quadriceps femoris muscle was evident within 4 weeks after hindlimb ischemia due to femoral artery ligation (Fig. 2A, arrowheads in the left panel). The temperature in the left ischemic limb increased gradually during the follow-up; however, it did not comparably recover to the level of the contralateral hindlimb (Fig. 2B). The ratio of skin temperature in the left hindlimb to that in the right hindlimb, the laterality in temperature, decreased to 0.50 ± 0.04 soon after ligation, followed by an elevation to 0.81 ± 0.02. In contrast, donepezil-treated mice did not suffer from severe muscular atrophy (Fig. 2A). The weight ratio of the left hindlimb to the right was 1.02 ± 0.04 ($P<0.05$, $n=10$) in donepezil-treated mice compared with 0.85 ± 0.01 ($n=10$) in control untreated mice (Fig. 2A). Furthermore, the laterality of temperature increased to 0.95 ± 0.01 with donepezil treatment ($P<0.01$ vs. control) (Fig. 2B). A pathological study revealed that, compared to untreated muscle (left in control, Fig. 2C), the number of nuclei in treated muscle increased along with more capillary-like structures (Fig. 2C). The number of nuclei per field in the donepezil-treated left hindlimb increased significantly compared to that in non-treated and ischemic hindlimbs (17.8 ± 1.4 vs. 8.6 ± 0.9, $P<0.01$, $n=9$). The immunohistochemical study showed that cells positive for